

distributions for both of the inelastic groups were expected to be isotropic. This was checked experimentally for the first group. The resulting cross sections were 0.187 ± 0.015 barn for the group to the first excited level, and 0.007 ± 0.002 barn for the second group. At the 1381-keV resonance the yield of the second group was measured at 90 degrees. The measured angular distribution was $1 - 0.45 \cos^2\theta$, and this was used to get the cross section from the differential cross section. The result was 0.0427 ± 0.0040 barn as the cross section for the second group.

The results of the angular distribution measurements are listed in Table II. All distributions were fitted with curves of the form $1 + a \cos^2\theta$; the coefficients a are listed. In addition, the angular distributions for protons to the 196-keV level at bombarding energies of 1355 keV and 1381 keV are shown in Figs. 11 and 12. The angular distribution data is meager, due to the difficulties involved in isolating the groups from elastically scattered groups. In addition, the 935- and 1431-keV resonances were not useful in attempting to determine the spins and parities of the two F^{19} excited levels as both are 1^+ levels formed by s -wave protons. The results are made more difficult to analyze due to the presence of the proton spin, making two outgoing channel spins possible in general.

Unique assignments for the excited levels of F^{19} could not be made on the basis of the inelastic proton results alone due to the reasons discussed above. However, measurements on the de-excitation gamma ray and on the $F^{19}(\alpha, \alpha')F^{19*}$ reaction did result in the assignments $\frac{1}{2}^-$ and $\frac{5}{2}^+$ for the first and second excited states respectively. These assignments are discussed in detail in an accompanying publication.²⁰ Our results are consistent with those assignments.

In conclusion we wish to express our appreciation to C. A. Barnes, R. F. Christy, R. Sherr, and J. Thirion for many discussions of these results.

Note added in proof.—In a recent paper, Dennison [Phys. Rev. **96**, 378 (1954)] has extended his original calculations³ on the tetrahedral alpha particle model of O^{16} and has made two different identifications of the theoretically predicted energy levels with those observed experimentally. In the first identification the 6.91-MeV level is identified with a 2^+ level of the first excited state of the triply degenerate normal mode of vibration of the alpha particles (ω_3). A 2^- level is not associated with this level. In the second identification, which corresponds to our previous discussion based on the original paper,³ the 6.91-MeV level is identified with a 2^+ level of the first excited state of the doubly degenerate mode of vibration (ω_2). In the light of these considerations, our results stand as a strong argument in favor of Dennison's first identification unless, as indicated above, the inversion frequency separating the 2^+ and 2^- states in the second identification is much larger than can be reasonably expected.

²⁰ Sherr, Li, and Christy (following paper).

Coulomb Excitation of F^{19} by Alpha Particles*

R. SHERR,[†] C. W. LI,[‡] AND R. F. CHRISTY

Kellogg Radiation Laboratory, California Institute of Technology, Pasadena, California

(Received August 16, 1954)

Gamma rays emitted in the excitation of F^{19} by α particles of 0.6 to 2.8 MeV have been studied. Resonances are found in the reaction $F^{19}(\alpha, p)Ne^{22*}$ at α particle energies greater than 1.3 MeV and in the inelastic excitation of 109-keV and 196-keV levels in F^{19} at energies greater than 2.2 MeV. At bombarding energies below 2 MeV, the cross sections for inelastic excitation of F^{19} decrease much too slowly for compound nucleus formation and are identified as being due to Coulomb excitation. The observed cross sections in the region 0.6 MeV to 2 MeV agree well with the theory for Coulomb excitation. The electromagnetic transition probabilities for decay of these states deduced from the excitation cross sections are in good agreement with those found from direct measurement of the lifetimes by Thirion, Barnes, and Lauritsen. Together with the results of Peterson, Barnes, Fowler, and Lauritsen on the inelastic excitation of fluorine by protons, these experiments lead to spin and parity assignment of $\frac{1}{2}^-$ for the 109 keV state and $5/2^+$ for the 196-keV state of F^{19} . The observed angular distributions of the γ rays from Coulomb excitation by α particles are also in accord with theory.

I. INTRODUCTION

ALTHOUGH extensive investigations of nuclear reactions in light nuclei have been carried out with protons and deuterons, relatively little work has been done with artificially accelerated α particles. In the present paper we wish to summarize our results on several reactions induced in F^{19} by α particles in the energy range 0.6 to 2.8 MeV. We have studied only

those reactions yielding γ radiation. These are the $F^{19}(\alpha, p)Ne^{22*}$ reaction leading to the excited state of Ne^{22} at 1.28 MeV ($Q=426$ keV) and the excitation of F^{19} states at 109 keV and 196 keV¹ in the reaction $F^{19}(\alpha, \alpha')F^{19*}$.

The first and second excited states of F^{19} are particularly interesting insofar as they are exceptionally

* Assisted by the joint program of the Office of Naval Research and the U. S. Atomic Energy Commission.

[†] On sabbatical leave from Princeton University.

[‡] Present address: Department of Radiology, City of Hope, Duarte, California.

¹ The energies of the low states of F^{19} quoted in this paper are somewhat lower than those in references 6–9 and reflect revised estimates based on private communication from R. B. Day, recent measurements by Mills, Hilton, and Barnes (unpublished); and new calculations of data of Peterson, Barnes, Fowler, and Lauritsen.

close to the ground state. The spin of the ground state is known to be $1/2$; this value has been considered anomalous in the usual coupling schemes in the $j-j$ model if one assumes the $1d_{5/2}$ orbit to have lower energy than the $2s_{1/2}$ or $1d_{3/2}$. Furthermore the simplest unmixed configuration $[(d_{5/2})^2; s_{1/2}]$ for F^{19} is excluded by the superallowed β decay of Ne^{19} . The determinations of the spins and parities of the nearby excited states may eventually clarify these questions.

The low states of F^{19} were first observed by Whaling and Mileikowsky² in the reaction $Ne^{21}(d, \alpha)F^{19}$. Day³ has found these levels in the inelastic scattering of neutrons by fluorine. The observation of their excitation by α particles has also been reported by Heydenburg and Temmer⁴ and by Jones and Wilkinson.⁵ These levels have been intensively studied in this laboratory by the inelastic scattering of protons, and their lifetimes have been measured. Summaries of these experiments and of the present results have been published in Letters to the Editor.⁶⁻⁹ The conclusions reached in the proton experiments are that the 196-kev state is $5/2^+$ and that the spin of the 109-kev state is $1/2$. The α particle work, in conjunction with the lifetime measurements, confirms the $5/2^+$ assignment, and leads to the assignment of odd parity to the 109-kev state.

We found no evidence for a 400-kev γ ray which could correspond to a reported state in Ne^{22} at 0.4 Mev.¹⁰ While we have used α particle energies up to 2.8 Mev, we observed no γ rays attributable to the reaction $F^{19}(\alpha, n)Na^{22}$. These last two (negative) findings are in agreement with the results of Heydenburg and Temmer.⁴ They also found no evidence of a 0.4-Mev γ ray. However they did observe a 592-kev γ ray at bombarding energies in excess of 3.05 Mev; they assign this γ ray to an excited state of Na^{22} at 592 kev. We did not look carefully for γ rays corresponding to the level at 3.4 Mev¹¹ in Ne^{22} which might have been excited at a bombarding energy as low as 2.06 Mev, but we found no indication of it in our spectra.

II. EXPERIMENTAL ARRANGEMENT

Singly charged helium ions were accelerated by an electrostatic generator. The ion beam impinged on the target after passing through a calibrated electrostatic analyzer of high resolution.

The γ rays were observed with a scintillation spec-

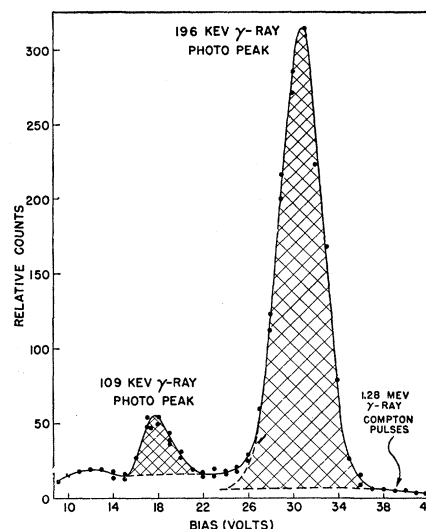


FIG. 1. Scintillation counter pulse height spectrum in the low-energy region produced by inelastic excitation of F^{19} by α particles. The target was a thick CaF_2 crystal and the bombarding energy was 2.35 Mev.

trometer¹² using a $NaI(Tl)$ cylindrical crystal $1\frac{1}{2}$ in. long and $1\frac{1}{2}$ in. in diameter. The pulse spectrum was analyzed with the aid of a 10-channel discriminator. A lead cylinder enclosed the counter fairly closely, leaving room however for an additional shield around the crystal. A house of 2-in. thick lead bricks was built around the entire counter-target assembly to improve the shielding, chiefly against low energy x-radiation coming from the generator.

Yield curves were obtained for a variety of thick and thin targets of CaF_2 , AlF_3 , and ZnF_2 . A typical low-energy scintillation spectrum is shown in Fig. 1; the target was a thick CaF_2 crystal and the bombarding energy 2.35 Mev. This spectrum was taken with a $\frac{1}{4}$ -in. copper cylinder around the crystal to remove lead fluorescent radiation which otherwise gives rise to a peak in the vicinity of 80 kev comparable with the 109-kev peak. The cross hatched areas of Fig. 1 were taken to represent the yields of the 109- and 196-kev radiation.

III. RESULTS

Resonances

Figure 2 summarizes the results of observations made with three thin targets. Here we were primarily interested in the location and magnitudes of resonances. The ordinates give the yield for the 1.28-Mev, 196-kev, and 109-kev radiations, while the abscissa is the energy of the incident beam. Target A was ZnF_2 evaporated onto a copper foil; target B was CaF_2 evaporated on copper; and target C was AlF_3 made by exposing an aluminum foil to HF fumes. The yields for target C were multiplied by $\frac{1}{3}$ for convenience in plotting.

In obtaining these points, the 10-channel discriminator was set to cover the 109-kev photopeak (see Fig. 1).

² C. Mileikowsky and W. Whaling, Phys. Rev. **88**, 1254 (1952).

³ R. B. Day, Phys. Rev. **89**, 908(A) (1953).

⁴ N. P. Heydenburg and G. M. Temmer, Phys. Rev. **94**, 1252 (1954).

⁵ G. A. Jones and D. H. Wilkinson (pre-publication report).

⁶ Peterson, Barnes, Fowler, and Lauritsen, Phys. Rev. **94**, 1075 (1954).

⁷ Thirion, Barnes and Lauritsen, Phys. Rev. **94**, 1076 (1954).

⁸ Sherr, Li, and Christy, Phys. Rev. **94**, 1076 (1954).

⁹ R. F. Christy, Phys. Rev. **94**, 1077 (1954).

¹⁰ B. J. Jolley and F. C. Champion, Proc. Phys. Soc. (London) **A64**, 88 (1951).

¹¹ F. Ajzenberg and T. Lauritsen, Revs. Modern Phys. **24**, 321 (1952).

¹² H. J. Woodbury, Thesis, California Institute of Technology, 1953 (unpublished).

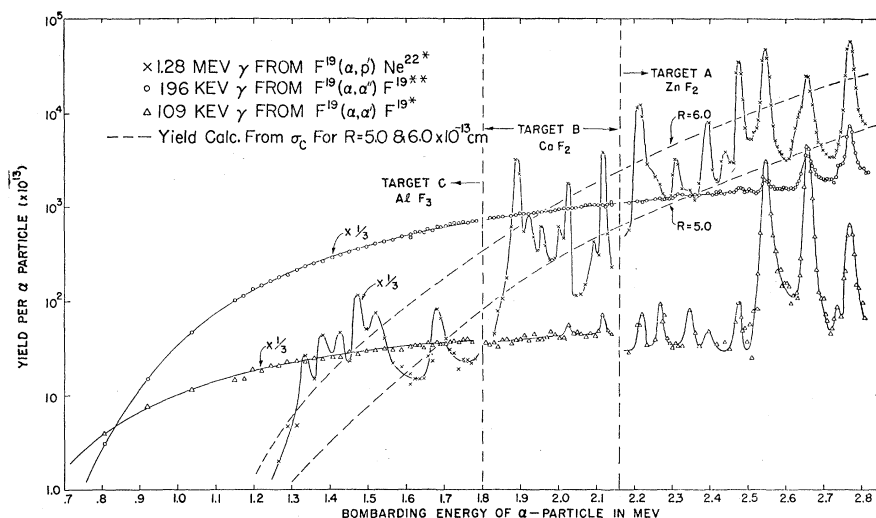


FIG. 2. Yield of the reactions $F^{19}(\alpha, p')Ne^{22*}$, $F^{19}(\alpha, \alpha')F^{19*}$ and $F^{19}(\alpha, \alpha'')F^{19**}$.

The 196-keV yield was obtained at the same time by taking the difference between two integral discriminators, one coinciding with the end of the 109-keV spectrum and the other set slightly beyond the 196-keV photopeak. The latter reading was taken as a measure of the yield of the 1.28-MeV γ ray. (The positions of the 1.28-MeV resonances were checked by observations on the 1.28-MeV photopeak using thin and thick targets.)

The observed counts were converted to yield per α particle, using the known calibration of the current integrator and approximate values for the scintillation counter efficiency for the various radiations. For the 196-keV data correction was made for the Compton pulses arising from the 1.28-MeV radiation which fell in the region of the 196-keV photopeak. This generally small correction was determined empirically using a Co^{60} source to give the shape of a pulse spectrum similar to that of the 1.28-MeV radiation in this region.

It is seen in Fig. 2 that the 196-keV curves for the three targets join smoothly. Recalling that the yields for target C were reduced by a factor of 3 in plotting, it is seen that the number of F atoms per unit area are in the approximate ratio of 1:1:3 for targets A:B:C. The target thickness was estimated to be 19, 15, and 33 kev (for A, B, C) at an α particle energy of 1.7 MeV.

It is estimated that the absolute scale of Fig. 2 is correct to 20 or 30 percent for the 1.28-MeV and 196-keV radiation. The absolute yield of the 109-keV radiation is much less certain as is evident from Fig. 2 at 2.16 MeV where the 109-keV curves for targets A and B should join. This discrepancy in yield reflects a major problem in determining the correct yield of the 109-keV radiation. This yield is quite small relative to that for the other radiations, except at the lowest energies.

Our procedure in finding the 109-keV yield was to draw a line joining the valleys above and below the peak in the pulse spectrum and to take the area above this line to represent the yield (Fig. 1). This procedure has the virtue of simplicity and reproducibility for a given geometry and choice of shielding. The apparent

magnitude of the 109-keV yield relative to the 196-keV yield was, however, quite sensitive to the geometry, target and shielding. In Fig. 3(a) we have plotted the 109-keV spectrum obtained with a thick CaF_2 target at a bombarding energy of 2.07 MeV with and without a $\frac{1}{4}$ -in. copper cylinder around the crystal. Using the procedure outlined above for finding the 109-keV photopeak area and comparing it with the corresponding 196-keV photopeak areas, we find for the ratio of the latter to the former, 12.1 with the copper shield, and 14.7 with the copper removed. It is clear that the $\frac{1}{4}$ -in. copper shield increases the number of 109-keV counts by back-scattering the γ rays which reach it, most probably the 196-keV radiation. For the measurements to be discussed below, we used 15-mil Ta foil to remove the lead x-rays which would otherwise be bothersome

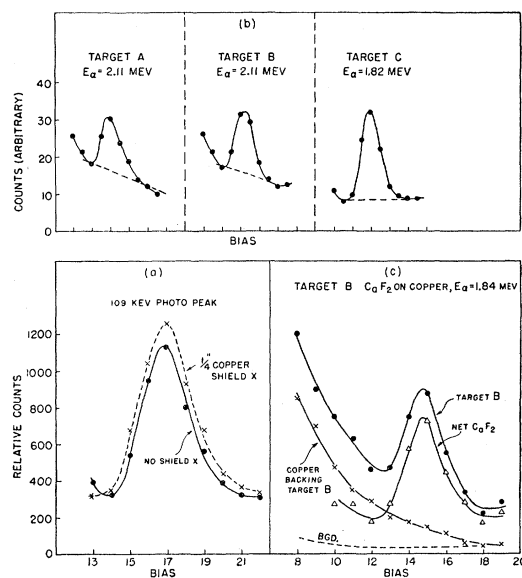


FIG. 3. Pulse height spectra in the neighborhood of 109 keV obtained under different conditions (see text).

when using thin targets. The tantalum shield gave spectra similar to the "no shield" curve of Fig. 3(a).

The choice of target also affected the analysis of the 109-keV γ ray. Figure 3(b) shows typical 109-keV photo-peaks obtained with targets *A*, *B*, and *C*. The dotted lines are the ones used in the analysis. It is evident that the copper-backed targets (*A* and *B*) exhibit a low energy radiation not attributable to fluorine. Figure 3(c) shows the spectra obtained from the front and back of target *B*; the copper backing is seen to contribute an appreciable continuous spectrum. This radiation is probably bremsstrahlung¹³ from the α particles. Mr. W. J. Karzas in this laboratory has calculated the bremsstrahlung to be expected and, finds approximate agreement with the data of Fig. 3(c). Thick CaF_2 and thin CaF_2 on Al gave spectra similar to that of target *C*.

In addition to the effects of shielding and target, there are also uncertainties arising from the low counting rates and from possible variations in width of the channels of the discriminator, especially those channels which register the valleys. The analysis is particularly sensitive to the latter, since the subtractions are relatively large.

The above remarks indicate the difficulties involved in an accurate determination of the yield of the 109-keV radiation. However, the yield of the bothersome radiations is smooth enough not to interfere with the detection of resonances for the 109-keV radiation.

The positions and yields of the resonances are tabulated in Table I. For the former we have taken the center of the observed peaks minus one half of the target thickness. All of the peaks observed have widths comparable with the (only approximately known) target thickness and therefore the true widths are less than, or comparable with, the target thickness. Additional correction for surface contamination might lower the resonance energies by 10 or 20 keV. The results of the present measurements are on the whole in good agreement with the observations of Heydenberg and Temmer.⁴

The rapid decrease of resonant yield of the 196- and 109-keV radiations relative to the 1.28-MeV yield with decreasing α particle energy is to be expected because of the much lower penetration factor for inelastically scattered α particles in comparison with that for the protons from the $\alpha-p$ reaction. The energy dependence (averaged over resonances) of the yield of the 1.28-MeV radiation is determined primarily by the penetrability of the incident α particle. The dotted curves in Fig. 2 correspond to the yield to be expected on the basis of the continuum theory if we assume the yield is determined by the cross section for formation of the compound nucleus:

$$\sigma_c = \pi \lambda^2 \sum_l (2l+1) T_l(E_\alpha),$$

where T_l is the transmission coefficient. The latter de-

TABLE I. Resonances in $F^{19}+\alpha$ reactions. E_α is the resonant α particle energy, E_c is the corresponding excitation energy in the compound nucleus Na^{23} if one uses 10.50 MeV for the mass difference $F^{19}+He^4-Na^{23}$. Columns 4, 5, and 6 list the peak yields per 10^{13} α particles for the 1.28-MeV, 196-keV, and 109-keV radiations; for the latter two the continuous yield has been subtracted. "U" marks unresolved resonances.

	E_α (Mev)	E_c (Mev)	Gamma-ray yields per 10^{13} α 's		
			1.28 Mev	196 kev	109 kev
Target C					
AlF ₃	1.315	11.59	79		
	1.362	11.63	128		
	1.408	11.66	138		
	1.455	11.70	345		
	1.501	11.74	225		
	1.662	11.87	245		
Target B					
CaF ₂	1.879	12.05	3140		
	1.914	12.08	817		
	1.948	12.11	607		
	1.994	12.15	606		
	2.017	12.17	1730		10
	2.083	12.22	420		
	2.109	12.24	3800		20
Target A					
ZnF ₂	2.207	12.32	12 000		40
	2.257	12.36	<i>U</i>	(100)	55
	2.298	12.40	3200		
	2.337	12.43	<i>U</i>		48
	2.383	12.47	8000		14
	2.428	12.50	3702		
	2.463	12.53	34 000	200	60
	2.533	12.59	46 000	400	3000
	2.648	12.69	24 000	1800	4500
	2.728	12.75	<i>U</i>	<i>U</i>	25
2.758	12.78	55 000	4700	600	

pends on the choice of a model. We have used the tabulations of Feshbach, Shapiro, and Weisskopf¹⁴ to evaluate σ_c for various values of the interaction radius. The two dotted curves shown in Fig. 2, correspond to radii of 5.0 and 6.0×10^{-13} cm. The correspondence of shape between the calculated and experimental curves is quite good. It is, of course, not possible to choose an interaction radius from this comparison. The smaller radius corresponds to one of the conventional prescriptions $(1.5A_1^{1/3} + 1.2) \times 10^{-13}$ cm, while the larger radius is given by $1.4(A_1^{1/3} + A_2^{1/3}) \times 10^{-13}$ cm. Qualitatively the latter might be preferred, since the penetrability for the outgoing proton would lower the theoretical yield curve, while the cross section for protons to the ground state (unobserved here) would raise the actual total yield.

Coulomb Excitation

The nonresonant yields of the 196-keV and 109-keV radiation at energies below 2.5 MeV vary much too slowly with energy to be ascribed to processes involving the barrier penetration of ingoing and outgoing α particles associated with formation of the compound nucleus. Results qualitatively similar to these were obtained by Heydenberg and Temmer⁴ and were ascribed to Coulomb excitation. In this process the

¹⁴ Feshbach, Shapiro, and Weisskopf, Nuclear Development Associates Report 158B-5 (NYO 3077) June 15, 1953 (unpublished).

¹³ C. Zupancic and T. Huus, Phys. Rev. **94**, 205 (1954).

incident α particle excites the F^{19} nucleus by virtue of the electromagnetic field associated with the passage of the α particle externally to the nucleus. From the yield curves we note that the cross section for formation of the compound nucleus, as inferred from the yield of the 1.28-Mev gamma ray, is comparable with the cross section for Coulomb excitation of the 109-kev level at as low an energy as 1.3 Mev. While the formation of the compound nucleus will not contribute directly to the excitation process (because of the extremely low probability that the α particle can escape), it might be expected to modify the calculation of the cross section for Coulomb excitation.

In order to compare the observed Coulomb excitation with theory, a series of measurements were carried out to determine the absolute cross sections accurately. Yield curves for the 196-kev and 109-kev radiations were taken with a semithick target (~ 100 kev) of CaF_2 evaporated on a 15-mil aluminum disk. At each energy a series of readings were taken with different channel settings of the multichannel discriminator in order to average out fluctuations in channel widths. These curves agreed in shape very closely (within 10 percent) with the curves for Target C (Fig. 3). Measurements were made at several energies with a Ta-lined lead collimator which restricted the passage of γ rays to be near the axis of the NaI crystal. With these "good geometry" measurements, the absolute yield was determined. In order to determine the absolute cross section, a target of CaF_2 was used whose width for protons was determined¹⁵ by observing the $F^{19}(p,\gamma)$ resonance at 873 kev. The width was found by comparing the integrated thin target yield with the yield of a (nearly) thick target.¹⁶ The corresponding number of F^{19} atoms was determined taking 11.9×10^{-15} ev cm² per F^{19} atom for the stopping cross section of CaF_2 for 880 kev protons. The error in the calibration due to uncertainty in target thickness and stopping power is probably less than 20 percent. The final results of these absolute determinations are shown in Fig. 4 in which the absolute cross section is plotted *versus* α particle bombarding energy (corrected for target thickness). For purposes of clarity, the weak resonances shown in Fig. 2 have been omitted. The curves in Fig. 4 are theoretical and will be discussed later.

Corrections for counter efficiency, absorption, and angular distribution were considered. We assumed that the photopeak areas measured the number of quanta entering the crystal (through the collimator). Although some of the 196-kev quanta give rise to Compton pulses, this loss is balanced by inscattering of gamma rays by the surroundings. A reasonable estimate would be that both are of the order of a few percent. The accuracy of the determination of the photopeak area of the 109-

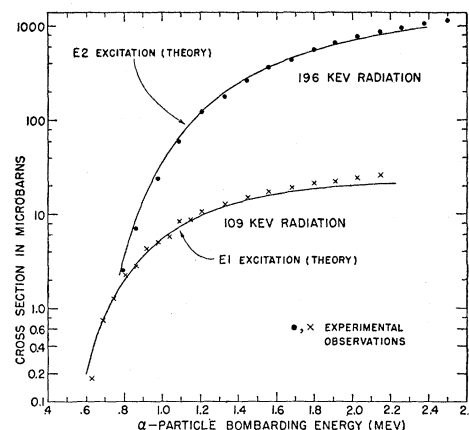


FIG. 4. Cross section for the inelastic excitation of the 109-kev and 196-kev states of F^{19} as a function of bombarding α particles energy. The points are experimental, the curves are theoretical.

kev radiation is more difficult to evaluate because of effects discussed previously. However, a comparison was made of the ratio of the differential yields of 196- and 109-kev radiations as determined from the thin-target data and from calibrated thick-target yields at 1.96 Mev. These agreed within 7.5 percent. Since the intensity of the 196-kev radiation relative to the 109-kev radiation varied by a factor of 1.5 between these two determinations, we estimate that the error in the photopeak area for the 109-kev radiation arising from improper allowance for the 196-kev spectrum is less than 20 percent at 2 Mev and is smaller at lower energies where the yields approach each other.

Absorption corrections were negligible, while for the effect of angular distribution we used the results of the next section (below). This latter correction was 14 percent for the 196-kev radiation and zero for the 109-kev radiation. In summary we estimate that the errors in absolute cross section are no larger than 25 percent for the 196-kev radiation and no larger than 35 percent for the 109-kev radiation.

In addition to the possible sources of error in the cross sections discussed above, there is also uncertainty in the correct value of E_α arising from the presence of surface deposits on the targets and from the lack of precise information regarding the thickness of the targets for α particles. The surface deposits may have been as thick as 10 to 20 kev with the result that the points may be plotted at too high an energy. The errors in target thickness (for α particles) is estimated to be ± 10 kev. The theoretical curves in Fig. 4 were chosen for best fit in the intermediate energy region to minimize this uncertainty in the energy scale.

Angular Distributions

Knowledge of the angular distributions of the 196-kev and 109-kev radiations relative to the α particle beam is necessary in order to establish the total cross sections. Furthermore, the theory for Coulomb excita-

¹⁵ We are indebted to Dr. C. A. Barnes and Dr. W. A. Fowler for preparation and calibration of this target.

¹⁶ Fowler, Lauritsen, and Lauritsen, *Revs. Modern Phys.* **20**, 236 (1948).

tion predicts the magnitude of the anisotropy to be expected for various spin assignments to the levels involved. The angular distributions predicted vary slowly with energy. Because of the low inelastic reaction cross section we investigated the yields at 0° , 45° , and 90° from a thick CaF_2 target at a bombarding energy of 1.84 Mev.

The CaF_2 was evaporated onto a 15-mil aluminum disk, which was then mounted in a lucite target chamber so that the target could be rotated about a vertical axis (the beam being horizontal). The counter was mounted on a stand which could be rotated around the target in a horizontal plane. A lead collimator (half-angle 10°) was mounted in front of the counter. The aperture-target distance was 2.0 in. Lead bricks were piled up to shield the counter as much as possible from the generator-produced background.

As a check on the geometry of the apparatus we used the angular distribution of the 478-keV gamma radiation produced in the inelastic scattering of α particles by Li^7 . The 478-keV level has spin $1/2$ and therefore the radiation should be emitted isotropically. Our procedure then was to bombard $LiOH$ which had been put on the back of the CaF_2 target, and measure the yield at 0° , 45° , and 90° . The target was then rotated through 180° and the yield for the fluorine was measured. (The target was placed at 45° to the beam so that the 0° and 90° positions were symmetrical with respect to the target.)

From the Li results we found that the yields at 90° and 45° were larger than the 0° yield by factors 1.04 ± 0.01 and 1.02 ± 0.02 respectively. These agreed with measurements of the geometry. We used these factors to correct the F^{19} results. For the 196-keV radiation the final results were $W(0^\circ)/W(90^\circ) = 1.22 \pm 0.02$ and $W(0^\circ)/W(45^\circ) = 1.08 \pm 0.03$, where $W(\theta)$ is the relative counting rate at an angle θ between the directions of the beam and the γ rays.

Using our usual prescription for finding the yield of the 109-keV radiation, we obtained $W(0^\circ)/W(90^\circ) = 1.09 \pm 0.06$ and $W(0^\circ)/W(45^\circ) = 1.08 \pm 0.08$. These results indicate a slight forward peaking. However, since the geometry for back scattering from the beam tube, target chamber, and shielding were not identical for the three angles, we investigated the back scattering effect. The pulses arising from the 196-keV radiation in the vicinity of the 109-keV photopeak can have their origin (a) externally to the counter assembly, (b) in scattering by the material surrounding the crystal, (c) in the crystal itself. Effects (b) and (c) would be the same for the three angles, while (a) would be expected to vary. Our procedure was to measure first the pulse spectrum with a $\frac{3}{16}$ -in. diameter disk of 30-mil Ta and 17-mil Cd placed directly behind the beam spot on the back side of the target. This absorber reduced the 196-keV radiation from the target by a factor of 4, and the 109-keV radiation by a factor of 400. The absorber was sufficiently small in diameter not to change

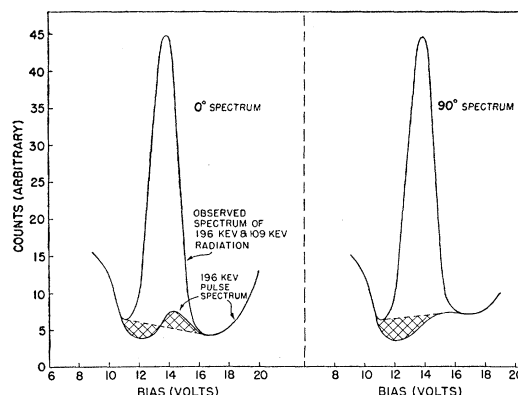


FIG. 5. Pulse height spectra (schematic) in the neighborhood of 109 keV obtained in the measurement of the angular distribution of the 109-keV radiation.

the amount of the backscattered radiation appreciably from its intensity in the angular distribution measurements. Thus the pulse spectrum obtained was that due to transmitted 196-keV radiation plus backscattered radiation from the surroundings. The measurements were repeated, with the same thickness of absorbers placed over the counter aperture to determine the magnitude of effects (b) and (c). Finally we reconstructed the pulse spectrum at 109 keV to be expected from the 196-keV radiation in the angular distribution measurements. The results are shown schematically in Fig. 5 for 0° and 90° . The dotted lines in each figure correspond to our standard prescription for finding the photopeak area. The cross-hatched areas indicate the errors in this procedure. For the 0° case it is evident that an underestimate on the lower side of the peak is practically balanced by an overestimate on the upper side. For the 90° case, however, our procedure leads to an underestimate of (9 ± 5) percent. No similar measurements were made at 45° , but from the appearance of the bias curve we feel justified in taking an intermediate value of (-5 ± 3) percent for the correction at 45° .

With these corrections the angular dependence is given by $W(0^\circ)/W(90^\circ) = 0.99 \pm 0.08$ and $W(0^\circ)/W(45^\circ) = 1.03 \pm 0.09$. Thus the emission of the 109-keV radiation appears to be isotropic. These results on the angular distributions of the 109-keV and 196-keV radiation will be discussed in the following sections.

IV. COMPARISON WITH THEORY

In this section we will discuss the theoretical Coulomb excitation functions to be compared with the experimental excitation functions of the 196-keV and 109-keV radiations at α particle bombarding energies below those which show pronounced resonance phenomena. We have compared the excitation of the 196-keV state with calculated electric quadrupole excitation of a $5/2^+$ state (the ground state of F^{19} is taken to be $1/2^+$). In the case of the 109-keV state, we have compared the

data with calculated electric dipole excitation of a $1/2^-$ state. We will also discuss magnetic dipole excitation of a $1/2^+$ state which is not, however, in accord with experiment.

The Electric Quadrupole Coulomb Excitation

We will use here the theory developed in the classical approximation ($2Z_1Z_2e^2/\hbar v \gg 1$) by Ter-Martyrosian¹⁷ and extended numerically by Alder and Winther.¹⁸ In the notation of Bohr and Mottelson,¹⁹ we have

$$\sigma = \frac{2\pi^2}{25} \frac{1}{Z_2^2 e^2} \left(\frac{Mv}{\hbar} \right)^2 B_{e\frac{1}{2} \rightarrow \frac{3}{2}} g(\xi), \quad (1)$$

where M is the reduced mass of the α particle and F^{19} , $Z_1=2$, $Z_2=9$, v is the relative velocity, and $\xi = (\Delta E/2E) \times (Z_1Z_2e^2/\hbar v)$. ΔE is the excitation energy in question (196 keV) and E is the bombarding energy. The quantity $g(\xi)$ has been calculated numerically and is given by Alder and Winther. In using this form for σ we note that the classical condition is fairly satisfactory since $2Z_1Z_2e^2/\hbar v > 8$ up to 2 MeV. However the additional requirement of the calculation, namely $\Delta E/E \ll 1$ is not sufficiently satisfied to give accurate results for $E \approx 1$ MeV. The extreme evidence of this failure lies in the way in which σ behaves in the neighborhood of threshold at 238 keV where σ should vanish exponentially, whereas ξ is finite as is $g(\xi)$. The simplest modification of the theory which introduces the proper exponential behavior at threshold is to replace ξ by $n_2 - n_1$, where $n_2 = Z_1Z_2e^2/\hbar v_2$, $n_1 = Z_1Z_2e^2/\hbar v_1$, and v_1 and v_2 are the relative velocities of colliding and separating nuclei respectively. Then

$$n_2 - n_1 = \frac{Z_1Z_2e^2}{\hbar} \left(\frac{1}{v_2} - \frac{1}{v_1} \right) = \frac{Z_1Z_2e^2}{\hbar} \left(\frac{v_1^2 - v_2^2}{v_1v_2(v_1 + v_2)} \right) \\ \approx \frac{Z_1Z_2e^2}{\hbar v} \frac{\Delta E}{2E} = \xi.$$

Thus for $\Delta E \ll E$, $n_2 - n_1 \approx \xi$ but near threshold, $n_2 - n_1 \rightarrow \infty$ and $g(n_2 - n_1) \rightarrow 0$ as it should. Although this substitution (which is suggested in ref. 17) produces presumably the correct exponential behavior near threshold, it could readily be in error by a power of $(n_2 - n_1)/\xi$. Consequently, we will assume our calculated σ to be in error by up to a factor of 2 around 1 MeV where $(n_2 - n_1)/\xi = 1.5$. On the other hand, compound nucleus formation is apparently relevant near 2 MeV, which can also modify the theory which neglects the finite nuclear size. Thus there is no energy range in which the existing calculations are entirely satisfactory for as light a nucleus as fluorine, and the

calculated σ will be presumed to contain errors of order a factor 2 either in absolute magnitude or in the ratio of σ at high to σ at low energy.

We have calculated σ from Eq. (1) with $n_2 - n_1$ replacing ξ . The calculations were fitted to the observed σ at ~ 1.4 MeV by suitable choice of $B_{e\frac{1}{2} \rightarrow \frac{3}{2}} = 7.8 \times 10^{-70}$. The resulting curve is shown as the solid line in Fig. 5. The agreement with experiment is good.

From the value of $B_{e\frac{1}{2} \rightarrow \frac{3}{2}}$ so determined we predict a value of the lifetime τ , since

$$\frac{1}{\tau} = T = \frac{4\pi}{75} \frac{1}{\hbar} \left(\frac{\omega}{c} \right)^5 B_{e\frac{1}{2} \rightarrow \frac{3}{2}},$$

$$B_{e\frac{1}{2} \rightarrow \frac{3}{2}} = (2/6) B_{e\frac{3}{2} \rightarrow \frac{1}{2}}.$$

There results a predicted lifetime $\tau = 2.5 \times 10^{-7}$ sec. This is in satisfactory agreement with the measured⁷ value $\tau \approx 0.8 \times 10^{-7}$ sec. The assumption of $3/2^+$ for the spin would have led to a predicted E_2 decay time τ less by a factor 1.5, and also in good agreement with the measured value. This possibility is, however, excluded by the argument in the next section.

The theory of Coulomb excitation also predicts the angular distribution of the γ rays. In this case, at a mean energy of 1.6 MeV we expect¹⁸ $W(\theta) = 1 + 0.67 B_2 P_2(\cos\theta) + 0.025 B_4 P_4(\cos\theta)$. For a $5/2^+$ state, $B_2 = 0.285$ and $B_4 = 0.381$. However, associated with the long lifetime, it has been found^{6,9} that the coefficient of $P_2(\cos\theta)$ is reduced by a factor of about 0.6; the coefficient of P_4 should show an even larger reduction of ~ 0.4 . The observed ratios $W(0^\circ)/W(90^\circ) = 1.22 \pm 0.02$ and $W(0^\circ)/W(45^\circ) = 1.08 \pm 0.03$ are consistent with the formula above if the reduction of the coefficient of P_2 is between 0.6 and 0.8. A $3/2^+$ state being excited and decaying by $E2$ radiation would also give an angular distribution consistent with experiment. However, if it decayed by $M1$ radiation the coefficient of P_2 would be negative, in disagreement with observation.

The value of B_e may be compared with a calculated one-particle (proton) matrix element for a $d_{5/2} - s_{1/2}$ transition, although we would not propose that the ground state configuration can be so simply treated. We get

$$B_{e\frac{1}{2} \rightarrow \frac{3}{2}} = \frac{e^2}{4\pi} \left(1 - \frac{Z}{A^2} \right)^2 \times \frac{6}{2} \times \langle i | r^2 | f \rangle^2.$$

Taking $\langle i | r^2 | f \rangle = \frac{3}{5} R_0^2$, we get a calculated R_0 from the experimental value of B . It is $R_0 \approx 5 \times 10^{-13}$, which is rather larger than conventional values for the nuclear radius, suggesting the possibility of some collective motion contribution to the matrix element.

The Electric Dipole Coulomb Excitation

The theory of the electric dipole excitation has been worked out by Mullin and Guth²⁰ and also by Ter-

¹⁷ K. A. Ter-Martyrosian, J. Exptl. Theoret. Phys. (U.S.S.R.) **22**, 284 (1952).

¹⁸ K. Alder and A. Winther, Phys. Rev. **91**, 1578 (1953).

¹⁹ A. Bohr and B. R. Mottelson, Kgl. Danske Videnskab. Selskab, Mat.-fys. Medd. **27**, No. 16 (1953).

²⁰ C. J. Mullin and E. Guth, Phys. Rev. **82**, 141 (1951).

Martyrosian.¹⁷ In this case, exact formulae²⁰ have been developed for $\sigma(\theta)$ and σ in the approximation that the finite size of the nucleus can be neglected. However, the exact formula involves hypergeometric functions which have been evaluated only in the limit $n_2 \rightarrow \infty$ (near threshold) and $n_2 - n_1$ small. The experimental data in this case extend from 600 kev where $n_2 - n_1 \approx 1$ to about 2 Mev where $n_2 - n_1 \approx 0.15$. The lower energy is still not low enough to make the threshold approximation good and at the higher energy the neglect of the finite size of the nucleus can hardly be accurate since compound nucleus formation is important. As a result, we again cannot apply the results of theory with high precision. We have, following Ter-Martyrosian, joined smoothly the limiting forms for σ in the comparison with experiment which was fitted at ~ 1.0 Mev. The resulting value of the dipole moment D^2 should be correct within a factor ~ 1.5 .

The electric dipole excitation has been calculated from the expression

$$\sigma = \frac{32\pi^2}{9e^2} \left(\frac{n_1}{Z_2} \right)^2 e^{-2\pi(n_2 - n_1)} B_{\frac{1}{2} \rightarrow \frac{3}{2}} f(E),$$

where $B_{\frac{1}{2} \rightarrow \frac{3}{2}}$ is the electric dipole operator as defined by Bohr and Mottelson. $f(E)$ is a slowly varying factor which approaches $\pi/\sqrt{3}$ near threshold and varies logarithmically with E at high energies; at 2 Mev it is ≈ 3 and varies approximately linearly with E between $\pi/\sqrt{3}$ and 3. The curve so calculated is shown as a solid line in Fig. 4. The correspondence with the experimental excitation function is quite good.

The value of $B_{\frac{1}{2} \rightarrow \frac{3}{2}}$ derived from this excitation function is $B_{\frac{1}{2} \rightarrow \frac{3}{2}} = 2.3 \times 10^{-30} e^2$. From this a lifetime τ can be predicted from

$$\frac{1}{\tau} = T = \frac{16\pi}{9} \frac{1}{\hbar} \left(\frac{\omega}{c} \right)^3 B_{\frac{1}{2} \rightarrow \frac{3}{2}}.$$

This gives $\tau = 2.1 \times 10^{-9}$ sec, whereas the directly measured lifetime $\tau = 1.0 \pm 0.3 \times 10^{-9}$ sec.⁷ The combined uncertainties in the two experiments, together with the approximations in the theory, are sufficient to account for the discrepancy of ~ 2 .

The observed angular distribution of the 109-kev γ ray is, of course, consistent with the spherical symmetry to be expected for a $1/2^-$ (or $1/2^+$) state. It also serves, however, to exclude the possibility that it is a $3/2^+$ state which is excited by $E2$ and decays by $M1$. Such a possibility would give $W(\theta) = 1 - 0.24 \cos^2 \theta$ which is inconsistent with observation.

The value of B can be compared to a calculated one-particle matrix element for a $p_{\frac{1}{2}} \rightarrow s_{\frac{3}{2}}$ transition for orientation purposes. We find

$$B_{\frac{1}{2} \rightarrow \frac{3}{2}} = \frac{3}{64\pi} e^2 \left(1 - \frac{9}{19} \right)^2 R_0^2,$$

which, for $R_0 = 1.4 \times A^{\frac{1}{3}} \times 10^{-13}$ cm, gives $B = 5.8 \times 10^{-28} e^2$ which is 250 times larger than the observed value. This

suggests that the transition involves the change of more than a single particle orbit.

In general it would be possible to determine the multipolarity of a Coulomb excitation from the shape of the excitation function. In the case of the 109-kev γ ray, however, in the range $0.6 \leq E \leq 2$ Mev this is not possible. The observed cross section is equally well represented by $E2$ excitation. Such an interpretation is not, however, possible because of the other experiments. It is discussed in the next section.

In ascertaining the parity of the 109-kev state, it is essential that the possibility of $M1$ excitation be discussed. Such excitation will proceed via the magnetic field of the moving α particle. The magnetic field is less than the electric field by a factor v/c and in the high-velocity realm, the magnetic excitation should be less than the electric by v^2/c^2 ²¹ if the magnetic dipole moment of the nucleus is substituted for the electric dipole moment. Thus, to fit the observed cross section would require a magnetic moment $\approx c^2/v^2 \approx 1000$ times the electric moment and a lifetime $\approx 10^{-12}$ sec. This latter value is in disagreement with observation.

V. DISCUSSION

In this section we review all of the experiments⁶⁻⁹ recently carried out in the Kellogg Radiation Laboratory on the low excited states of F^{19} .

The assignment of $5/2^+$ as the spin of the 196-kev state of F^{19} is relevant to the further discussion of the problem, so its basis is outlined below. First, the 196-kev gamma-ray angular distributions from the inelastic scattering of protons at the 2^- resonances in Ne^{20} lead to $5/2^+$ assignment. A $3/2^+$ state decaying by magnetic dipole radiation would require the coefficient A_γ in $1 + A_\gamma \cos^2 \theta$ to be zero or negative in contradiction to the experimental data. On the other hand, the $E2$ decay of a $3/2^+$ state would give $0 \leq A_\gamma \leq 14/22$ which is consistent with the data. ($3/2^+$ is also consistent with the angular distribution observed in Coulomb excitation.) The angular distribution for $E2$ decay of $5/2^+$ state is also consistent with the data. On a *priori* grounds, a $3/2^+$ state should decay by $M1$ radiation in about 10^{-11} sec compared to 10^{-6} to 10^{-7} sec by $E2$ decay so that the assumption of $E2$ decay of a $3/2^+$ state implies a forbiddenness of $M1$ decay by a factor $\sim 10^4$ which is very unlikely. The measurement of the lifetime of 10^{-7} sec confirms the assumption that the state is decaying by $E2$ radiation. Finally, the cross section for Coulomb excitation is in good numerical agreement with the observed lifetime if $E2$ excitation and $E2$ decay are assumed. In principle this agreement could distinguish between $3/2^+$ and $5/2^+$ since there is a difference of a factor of $6/4 = 1.5$ in the statistical weights. However, the inaccuracies in present theory of the excitation process probably preclude such a fine

²¹ K. Alder and A. Winther have calculated the magnetic dipole excitation and find it given by $0.055v^2/c^2$ times the expression for electric dipole excitation (private communication).

distinction. In conclusion, the facts on the 196-kev state are most reasonably explained by a $5/2^+$ assignment, which, moreover, is expected from the shell model. It should be noted, however, that a $3/2^+$ assignment is not directly disproved but only made unreasonable by the fact that the $M1$ transition to the ground state (and also the transition to the 109-kev state) would have to be suppressed by apparently accidental factors of many powers of ten. Since a $3/2^+$ assignment for the 196-kev state at best makes the explanation of the 109-kev state only more difficult, it will not be considered further.

In discussing the 109-kev state we note that the lifetime of 10^{-9} sec requires that the transition be dipole. The expected lifetime for an $E2$ transition would be about 10^{-5} sec, whereas the lifetime for $E1$ could be 10^{-11} to 10^{-12} sec and for $M1$ it could be $\sim 5 \times 10^{-11}$ sec. Thus the spin of this state must be $1/2^\pm$ or $3/2^\pm$. Since the unexpected feature of these assignments is the negative parity, the real problem is to decide if $1/2^+$ or $3/2^+$ is possible. If these are not reasonable, then $1/2^-$ is the only choice since the $3/2^-$ would permit the cascade 87-kev γ ray at too rapid a rate and would not automatically give isotropy to the γ rays.

The $1/2^+$ Possibility

This assignment would be in satisfactory agreement with the lifetime for decay and with the isotropy of the γ rays. However, the Coulomb excitation can then not be understood. From the lifetime, we can compute the $M1$ matrix element. Coulomb excitation by α particles of a $1/2^+$ state should be smaller than the $E1$ excitation by a factor $\sim 10^4$ for the same dipole moment. Consequently, the state cannot be excited as observed by magnetic Coulomb excitation and the spin is not $1/2^+$.

The $3/2^+$ Possibility

The decay must be predominantly $M1$. On the other hand, as we see above, the excitation must be $E2$.

From the Coulomb excitation cross section, we calculate the (matrix element)² as 35 times smaller than for the 196-kev transition (the fit to the data is fairly good to ~ 1.5 Mev). Thus the calculated $E2$ lifetime would be $35/1.5 \times (196/109)^5 \times 2 \times 10^{-7}$ sec so $\tau(E2)$ would be 7.7×10^{-5} sec. As a result, the ratio of $E2$ to $M1$ in the decay is $1.0 \times 10^{-9}/7.7 \times 10^{-5} = 1.3 \times 10^{-5}$. Thus the $E2$ admixture would perturb the calculated angular distributions for the $M1$ decay by only ~ 1 percent, which is negligible. We are left with a direct contradiction with experiment in the angular distribution of the 109-kev radiation as given by Coulomb excitation. The observed distribution is spherical and cannot be brought into agreement with $1 - 0.25 \cos^2\theta$ calculated for $E2$ excitation and $M1$ decay. Further, the expected $M1$ decay rate for the $5/2^+ \rightarrow 3/2^+$ 87-kev transition would be 10^{10} sec⁻¹. It is observed to be $\leq 10^8$ sec⁻¹, a discrepancy of at least 10^5 ; this is also regarded as a major failure of this supposition. Finally the universal isotropy of the 109-kev radiation finds no explanation, although isotropy from a $3/2^+$ state formed from a 2^- resonance is a possible result.

The $1/2^-$ Possibility

This assignment explains both the isotropy of the radiation and the lack of the 87-kev transition ($5/2^+ \rightarrow 1/2^-$ would be $M2$ with a transition rate $\sim 10^8$ sec⁻¹). In addition, however, the fact that the lifetime calculated from $E1$ excitation agrees with that observed is an exceedingly strong argument in its favor.

In conclusion we think the only reasonable explanation of the facts is that the states are $5/2^+$ and $1/2^-$, taking the ground state to be $1/2^+$.

The authors take pleasure in acknowledging the many discussions of these problems with C. A. Barnes, W. A. Fowler, C. C. Lauritsen, and J. Thirion of the Kellogg Radiation Laboratory.